Available online at www.sciencedirect.com

ScienceDirect

Procedia CIRP 91 (2020) 113–120

www.elsevier.com/locate/procedia

30th CIRP Design 2020 (CIRP Design 2020)

Computer aided modelling and experimental validation for effective milling operation of titanium alloy (Ti6Al4V)

*Isaac Tlhabadira[a], Ilesanmi Daniyan[b], Leonard Masu[c], Khumbulani Mpofu[b]

[a]*Department of Mechanical & Mechatronics Engineering,Tshwane University of Technology, Pretoria 0001, South Africa.*
[b]*Department of Industrial Engineering,Tshwane University of Technology, Pretoria 0001, South Africa**
[c]Department of Mechanical Engineering, Vaal University of Technology, Vanderbijlpark, South Africa.

*Corresponding author. Tel.: +27670360861 *E-mail address:* itlhabadira@gmail.com

Abstract

Titanium alloy (Ti6Al4V) is characterized with excellent mechanical properties, which makes it suitable for many industrial applications. However, the poor rate of machinability mitigates the use of titanium alloy (Ti6Al4V). This study highlight the various methods to improve the machinability and surface finish of titanium alloy. These methods include; the use of PCD and PCBN tools, cooling systems, process optimization as well as the design and selection of the proper geometry for the cutting tool. The Computer Aided Design, modelling and simulation as well as the Finite Element Analysis of the milling process of Ti6Al4V was carried out using Solidworks 2016. The physical experiments were conducted on a DMU80monoBLOCK Deckel Maho 5-axis CNC milling with the stationary dynamometer (KISTLER 9257A 8-Channel Summation of Type 5001A Multichannel Amplifier) mounted directly to the machine table and the work piece screwed to it. The milling operations was carried out with different combination of cutting parameters while the values of the cutting force for each of the experimental trial was collected through the Data Acquisition System (DAS) connected to the computer. The results obtained show that the process parameters affect the magnitude of the cutting force significantly which in turn affects the rate of material removal. This work finds application in the manufacturing industry as it provides in depth understanding of the machining characteristics and behaviour of titanium alloy.

Keywords: chatter; cutting tool; process optimization; Titanium alloy; vibration

1. Introduction

Titanium alloy (Ti6Al4V) is characterized with excellent mechanical properties such as its high strength to weight ratio, high corrosion resistance, high stiffness and good formability, which makes it suitable for many industrial applications in a bid to reduce the energy consumption and increase the environmental friendliness of the final product. Titanium alloy (Ti6Al4V) finds application in some industrial applications such as in biomedical, aerospace, automotive, marine, mining, railway and more [1].

Nomenclature

$\boldsymbol{\beta}$	Helix angle
$\boldsymbol{n}$	Number of teeth
$\boldsymbol{\beta_1}$	Axial rake angle
$\boldsymbol{\beta_2}$	Radial rake angle
$\boldsymbol{\alpha}$	Cutting edge angle
$\boldsymbol{\theta}$	Clearance angle
φ	Relief angle

10.1016/j.procir.2020.03.098

However, some identified limitations mitigate the use of titanium alloy (Ti6Al4V). For instance, its low Young's modulus and high strength often lead to vibration and subsequently chatter [1]. Furthermore, its weak thermal conductivity can cause chemical reaction at high temperature (above 500°C) resulting in the formation of built up edges. With less of plastic deformation at high temperature, the material is prone to adiabatic failure and high strain rate machining can result in the formation of adiabatic shear bands.

These limitations can result in surface damage, excessive flank wear and consequently, in poor surface finish. Poor surface finish is detrimental to a product development in that it can affect its dimensional accuracies, as well as the quality and performance of the final product [2-4]. The classes of titanium alloys include; alpha (α), alpha-beta (α-β) and beta (β). The near-beta titanium alloys have a poor machinability compared to the alpha-beta (α-β) Ti alloys, hence, the alpha-beta (α-β) find extensive application in the automobile and aerospace industries for the development of automobile and aircraft components such as the airframes and engine components [5-8]. On the other hand, the β alloys find application in high strength applications due to its good formability [9]. The "α" phase of Ti-6Al-4V has a hexagonal closely packed (HCP) crystalline lattice structure while the "β" phase has a body centred cubic (BCC) crystalline lattice. The "α-β" phase combination changes at 980°C at a point known as the "β" transition temperature. Above this temperature, the alloy exists only in the BCC "β" phase. Research have proven that the high strength and poor thermal conductivity of titanium alloy contribute to its poor machinability [10-12]. The low thermal conductivity often leads to formation of shear bands that can cause temperature to build up at the tool-work piece interface. When high temperature builds up at the work-tool interface, it may cause the chips to build up edges, resulting in poor surface finish. In addition, an increase in temperature often increases the cost and energy requirement of the cutting process thereby making the process less environmentally friendly. Most research on titanium machining were reported on low speed machining with a very few reported works on high speed machining mainly due to increase of tool-work interface temperature. High speed machining of titanium alloy with high temperature can induces severe tool wear and deteriorates the surface finish. In addition, researchers are still exploring different approaches for the development of an efficient process for machining titanium alloy in order to mitigate its machinability challenges. Most importantly, the development of computer aided modelling and simulation based approach has not been sufficiently reported by the existing literature. The numerical approach used in this study will allow proper study of the machining operation in a virtual environment in order to avoid expensive rework. This will also enhance the determination of the optimum ranges of the process parameters to promote effective machinability of titanium alloy. This work finds application in the manufacturing industry as it provides in depth understanding of the machining characteristics and behaviour of titanium alloy.

2. Methodology

The methodology employed in this work include the process design which involves the analysis of the suitability of the cutting tool for the required operation as well as the determination of the critical process parameters. It also include the analysis of the cooling systems and the chances of modulation during the machining operation. Next is the numerical experimentation involving the computer aided design, modelling, simulation of the cutting process as well as the finite element analysis of the work piece during the machining operation. This is followed by the use of the design of experiment tools for the feasible combination of the physical experiments and the conduction of the physical experimentations. The chemical composition as well as the mechanical and electrical properties of the titanium alloy (Ti-6Al-4V) are presented in Tables 1 and 2 respectively.

Table 1. Chemical composition of titanium alloy (Ti-6Al-4V) [13].

Element	Al	Fe	O	Ti	V
Percent weight (wt.%)	6	0.25	0.2	90	4

Table 2. Mechanical and electrical properties of titanium alloy (Ti-6Al-4V) [13].

S/N	Properties	Value
1.	Mechanical	
2.	Density	45000 kg/m^3
3.	Brinell's hardness	334
4.	Yield strength	830 MPa
5.	Ultimate tensile strength	950 MPa
6.	Bulk modulus	150 GPa
7.	Modulus of elasticity	113.8 GPa
8.	Poison's ratio	0.342
9.	Shear modulus	44 GPa
10.	Shear strength	550 MPa
	Electrical	
1.	Specific heat capacity	0.5263J/g°C
2.	Thermal conductivity	6.7 W/m.K
3.	Melting point	1660°C
4.	Coefficient of Thermal expansion	8.70 K^{-1}

The low modulus of elasticity of titanium is the main cause of chatter during machining. This causes deflection when subjected to cutting pressure and the spring-back induces cutting edge failure and vibration [14]. Furthermore, the growth of flank wear grows linearly between 20 to 200 m/min of cutting speed for Ti6Al4V and for 250 m/min the flank wear growth found to have an exponential increase [15]. Fig. 1 illustrates the mechanics of milling cutting operation.

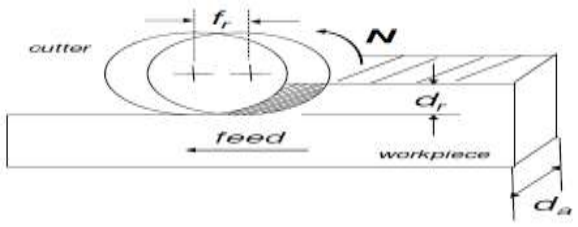

Fig. 1. The mechanics of milling cutting operation [16].

2.1 Process design

The machinability and surface finish of Ti alloy can be improved in the following ways;

i. The use of PCD and PCBN tools

The Polycrystalline Diamond (PCD) and Polycrystalline Cubic Boron Nitride (PCBN) cutting tools and inserts have greater hardness than the titanium alloy as well as high toughness, wear resistance, thermal conductivity and lower coefficient of friction. The geometry of the tool can be optimized with the appropriate edge preparation, radius, rake angles, wipers and chip breakers to meet the surface finish and dimensional tolerance requirements of the work piece (Ti6Al4V).

ii. Cooling systems

Rahman *et al.* [3] and Yang and Liu [17] proposed the use of high-pressure coolant (40 kPa, water jet coolant) to enhance the lubrication and cooling at the tool-work interface. The introduction of cooling systems during machining operation of titanium alloy will eliminate the adhesion of work material on the cutting edge and improves the tool life as well as the surface finish.

iii. The use of Modulation Assisted Machining (MAM)

The MAM process promotes a controlled oscillation during the machining process to improve the machining conditions. This improves process efficiency, precision and capability most especially in difficult-to-machine materials such as the titanium alloy, that are required for high-performance operations. The MAM process incorporates fundamental changes in mechanics of chip formation and fluid access to machining interfaces. A preliminary success on machining titanium alloys was reported with the use of MAM [18].

2.2 Process optimization

The process optimization involves the determination of the most feasible combination of the values of the process parameters that will produce the least deflection, vibration, surface roughness and friction with good machinability and process economics. The process parameters include; the cutting speed, feed rate, depth of cut, spindle speed, cutting force, temperature etc. The effective control of process parameters during the milling operation of Ti6Al4V will help to obtain a product that conforms to machining requirements. In addition, a good process design will also assist in the selection of the best possible combinations of process parameters, which will significantly improve the manufacturing economics in terms of cost and production time. To determine the optimum range of the process parameters, the Design of Experiment (DoE) are often carried out with the aid numerical experimentation via the Response Surface Methodology (RSM), Artificial Neural Network (ANN), Taguchi, Generic Algorithm (GA) etc.

i. Depth of cut

The depth of cut is the perpendicular distance measured between the machined surface and the uncut surface of the work piece, which is a function of the thickness removed from the work piece during the machining operation. As the depth of cut increases within its optimum range, the surface area to volume ratio decreases, hence, the friction and energy requirement of the process decreases. The reduction in friction and energy requirement of the process reduces the temperature at the tool-work piece interface, thus, making the process more environmentally friendly. This can also promote significant improvement in the quality of surface finish and the dimensional accuracy of the final product.

ii. Cutting speed

The cutting speed is the relative velocity between the cutting tool and the work piece during engagement for material removal. Within the optimum range of the cutting speed, an increase in the cutting speed will result in the reduction in the cutting force, machining time, friction and energy requirement of the process, thereby, promoting the development of work piece with smooth surface with the reduction in chip thickness due to the thermal softening.

The cutting speed is expressed as Equation 1.

$$V = \frac{\pi DN}{1000} \quad (1)$$

Where D is the diameter of the work piece (mm) and N is the spindle speed (rpm).

iii. Feed rate

The feed rate is the measure of the relative velocity moved by the cutting tool along the work piece in one revolution per minute. Within the optimum range of the feed rate, an increase in the feed rate will result in quick material engagement and removal. This is because an optimum feed rate leads to increase in the length of the work piece with the production of chip and work piece with reduced surface roughness and chip thickness.

The feed rate (V_f) is expressed as Equation 2.

$$V_f = n \times f_z \times Z \quad (2)$$

Where; n is the number of teeth and f_z is the feed per tooth (mm/tooth), and Z f_r is the number of flutes.

2.3 Determination of optimum cutting tool geometry

The design requirements of a high performance milling cutters takes into consideration the geometry, which is key to the surface finish requirement of the work piece. The geometry of the cutting tool for the up and down milling operation is shown in Fig. 2.

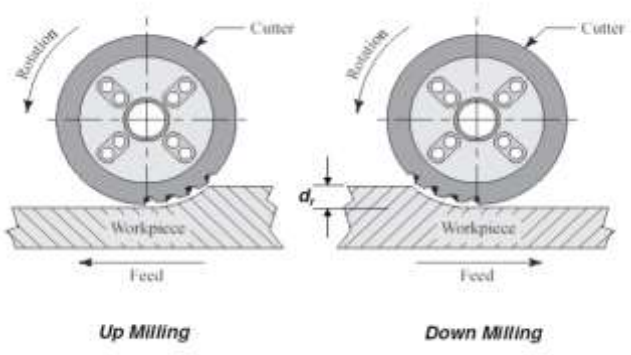

Fig. 2. The orientation of the cutter for up and down milling operation [16].

The high performance milling cutters should be designed to have unequally paced cutting edges as well as uneven helical pitch in order to reduce vibrations and enhance smooth cutting action. The design should also incorporate high cutting performance at high speed and temperature. Because of high temperature, it is recommended that the tool be coated to prevent oxidation and supplemented with an optimized fine-grain substrate for improved toughness and hardness. The cutter should also be designed such that its geometry will allow sufficient space for chip evacuation from the tool-work piece interface. Also, the design should consider the homogeneity of the cutting edge and should be rounded off to prevent the growth of cracks and chips as well as rate of wear while ensuring slow and even abrasion.

i. The helix angle

This determines the surface finish, vibrations and deflection of the work piece. Large helix angle of a mill cutter often leads to minimal vibration and quick chip removal. On the other hand, the cutting tool becomes weaker with reduction in its useful life. However, smaller helix angle makes the cutting tool stronger but with increased surface roughness. Hence, smaller helix angle are suitable for heavy cut where surface finish is not important while larger helix angle are often desirable for finishing operations.

ii. The lead angle

The lead angle is the approach angle of the cutting edge with respect to the work piece, which is measured off the cutter axis. Hence, as opposed to the small lead angle, a large lead angle will bring about a significant increase in chip thickness, reduction in the overall contact area with decrease in the tool life. This however will enhance quick material removal rate with the overall reduction in the machining time.
The lead angle is expressed by Equation 3.

$$Lead\ angle = \frac{Cutter\ diameter \times pi}{Tangent\ helix\ angle} \quad (3)$$

iii. The rake angle

The rake angle represents the angle of inclination of the top surface of the cutting edge measured in the axial or radial planes. Milling cutters with higher positive rake will consume less power than negative axial rake or lower positive rake angles. Also, the cutting edge of the tool can be strengthened using a negative but radially raked cutting tool which allows for the optimization of the cutting speed and tool life.

iv. The number of flutes

Deep polished flutes are characterized with sharp cutting edges and suitable for cutting soft materials like aluminum producing large amounts of chips, hence, large number of flutes may cause the frequent collision of the flutes with the formed chips thereby causing chatter. Meanwhile, tough materials like the titanium alloy often require shallow flutes and square off cutting edges to facilitate improved tool life and effective rate of material removal. The more the number of flutes, the more the cutting edge and the narrower the space for quick chip removal. Hence, since the flute space reduces with increasing number of flutes, thus, an important design decision is the selection criteria involving the choice of the right number of flutes with respect to the chip loads. The use of 2-flutes enhances the largest amount of flute space thereby allowing for quick chip removal in soft materials. On the other hand, 3-flutes allows for better finish in harder materials and provides greater strength than the 2-flutes. Hence, the 3-flutes is more suitable for slotting operations in both ferrous and non-ferrous materials. The use of 4-flutes (multiple flutes) often allows for faster feed rate, which enhances good surface finish. However, the reduced flute space may hinder quick chip removal, hence, it is most ideal for finishing operations requiring light cutting with small amount of chip loads.

2.4 Numerical experimentation

The Computer Aided Design (CAD), modelling and simulation of the milling operation was carried out using the Solidworks 2016. The Finite Element Analysis (FEA) was also carried out in order to study the engagement of the cutting tool with the work piece. The essence is to understudy the behaviour of the material to stress, strain and deformation distribution. The mesh type (10 elements) with an average element size $20 \times 20\ \mu m$ with linear displacement and temperature advancing front was employed. This is to mesh the cutting tool and the work piece into finite elements. It was thereafter subjected to convergence simulation runs with mesh refinement feature used for the ease of convergence. The operating temperature corresponds to 200°C in a thermal step within a step time of 10 milliseconds while the thermal boundary conditions were imposed axis of the model. The temperature of the node however is constrained to the ambient (20°C).

2.5 Physical Experiment

The physical experiment was conducted on a DMU80monoBLOCK Deckel Maho 5-axis CNC milling. The stationary dynamometer (KISTLER 9257A 8-Channel Summation of Type 5001A Multichannel Amplifier) was mounted directly to the machine table with the work piece (Titanium alloy) screwed to it. The milling operations was carried out with different combination of cutting parameters of cutting speed, feed per tooth and depth of cut as given by the Central Composite Design (CCD). The CCD is an experimental design approach in the Response Surface Methodology (RSM) and was employed for this work due to the iterative nature of the physical experimentations. The approach has been proved to be suitable for sequential and iterative experimentations as well as the experimental matrix design for the feasible combinations of the process parameters [21-23]. The feasible range of the process parameters were selected after extensive literature survey involving a careful study of similar works carried out by previous researchers [24-26]. The values of the cutting force for each of the experimental trial was collected through the Data Acquisition System (DAS) connected to the computer. The illustration of the experimental set up is shown in Fig. 3.

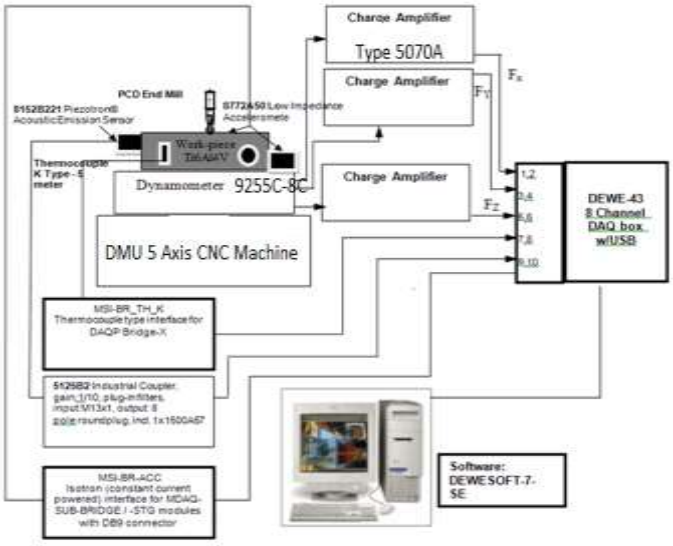

Fig. 3. The dynamometer set up for cutting force measurement [20].

The specifications of the cutting tool is presented in Table 3.

Table 3. The cutting tool specifications.

Symbol	Parameter	Value
T_d	Tool diameter (mm)	10
F_l	Flute length (mm)	15
F_n	Number of flute	2
L	Overall length(mm)	58
β	Helix angle (°)	30
n	Number of teeth	2
β_1	Axial rake angle	15°
β_2	Radial rake angle	15°
α	Cutting edge angle	10°
θ	Clearance angle	10°
φ	Relief angle	10°

3. Results and Discussion

Fig. 4 shows the results of the stress distribution of the titanium alloy during milling operation. The stress induced in the material ranges from a minimum value of 539 Pa to maximum value of 16.42 MPa. The maximum value of the stress induced is significantly lower than the yield strength of the material, thus, indicating low rate of material removal. This is because the applied cutting force is insufficient to bring about sufficient shearing action. However, the stress induced was observed to be maximum around the shear plane. This is the point at which the cutting tool engages the work piece resulting in work piece deformation via the shearing action of the cutting tool. The magnitude of the stress at point is connected with the fact that temperature increase more around the shear plane due to the engagement of the cutting tool and the work piece resulting in the buildup of stresses. The results obtained were similar to the findings of Priyadarshini et al. [27] during the finite element modeling of chip formation in orthogonal machining.

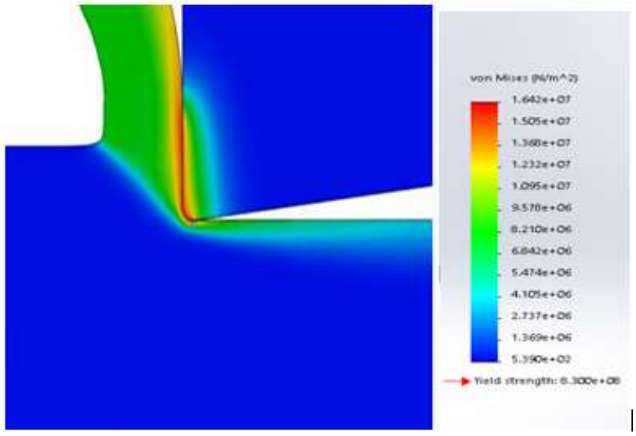

Fig. 4. Stress distribution.

Fig. 5 shows the displacement distribution of the material. The displacement distribution of the material under the application of cutting force is a function of the rate of stability of the process. When the cutting force exceeds the threshold value, the material and work piece are displaced due to increase in vibration and chatter with increasing surface roughness of the final product. The magnitude of the displacement ranges from a minimum value of $1.0 \times 10^{-30}\ mm$ to $2.891 \times 10^{-2}\ mm$. The small value of displacement may indicate the application of low cutting force or adequate clamping of the work piece and cutting tool.

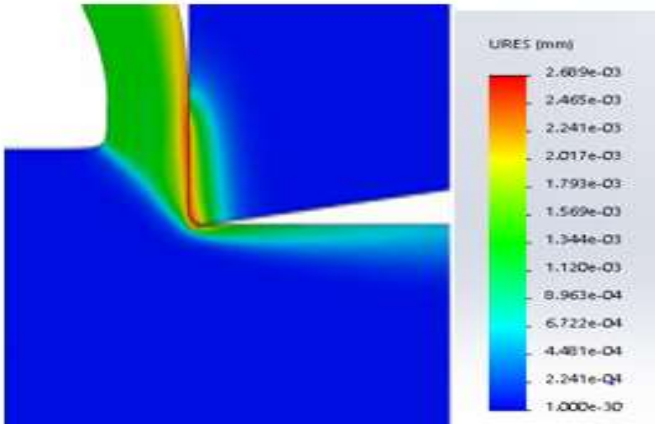

Fig. 5. The displacement distribution.

Fig. 6 shows the strain developed in the material as a result of the stress induced. The strain distribution represents the change in the dimensions or orientation of the material under the application of cutting force which is a function of the rate of material's deformation. The magnitude of the strain ranges from a minimum value of 1.128×10^{-8} to 9.228×10^{-5}. The small value of strain indicates insignificant material removal with the applied cutting force having little impact on the dimensions and orientation of the material.

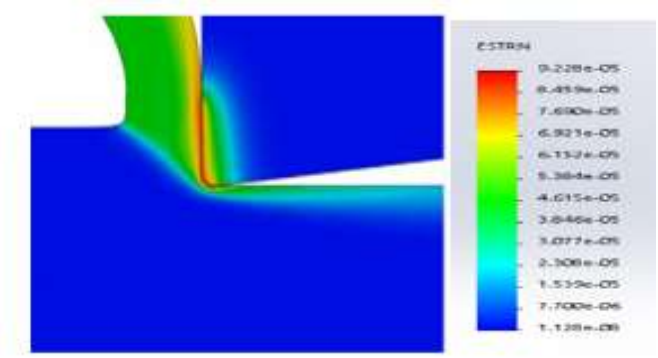

Fig. 6. The strain distribution.

Table 4 presents the radial, tangential and axial cutting forces in the X, Y, and Z directions for various combinations of the process parameters. The effect of the process parameters as it affects the variations in the cutting forces were studied. The measurement of the cutting force allows for the process optimization of the milling process as well as the development of a mathematical model for the prediction of the cutting force. The cutting forces are exerted in three directions namely the tangential, radial and axial directions. The tangential force is the force which overcomes the resistance to rotation and cutting hence it accounts for a greater proportion of the cutting force as shown in Fig. 4. The rake angle plays significant role in the determination of the cutting force as it determines the depth of cut, power required for the cutting operation as well as the strength of the cutting edge and chip flow direction. The axial rake angle determines the direction of chip disposal and produces excellent machinability when positive while negative rake angle produces excellent chip disposal. The cutting force increases as the rake becomes more negative with an increase in the strength of the cutting edge of the tool. In addition, the lead angle of the tool which measures the angle at which the cutting edge of the tool approaches the work piece influences the magnitude and direction of the radial and axial cutting forces. This also determines the thickness of the chip. Hence, small angle of the lead angle produces thin chips and small cutting impact, thus, the impact of the cutting force and chip thickness increases as the lead angle increases.

Fig. 7 shows the variation of cutting forces within 20 seconds. It was observed that the value of the tangential cutting force (Fx) was the highest followed by the radial cutting force while the axial cutting was the least.

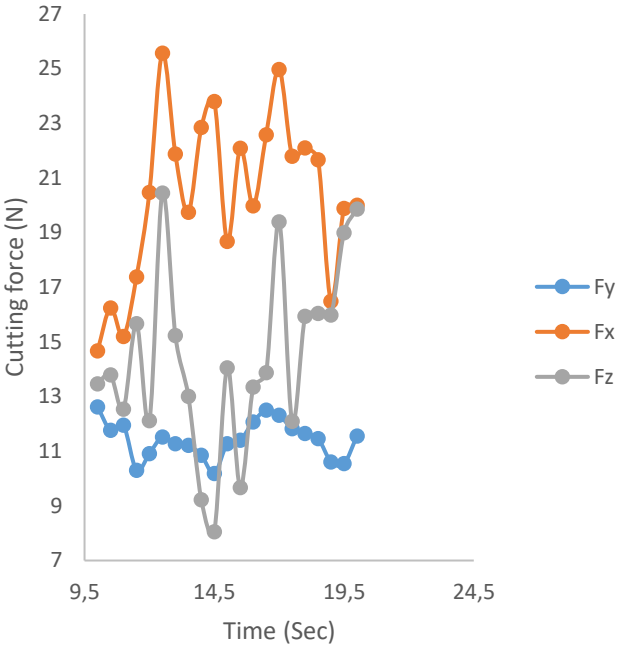

Fig. 7 The variation of cutting force with time.

Fig. 8 shows the variation of the moment of the cutting forces within 20 seconds. It was observed that the value of the moment of force has the highest magnitude along the radial axis, followed by the axial axis and the least values of the moment of forces was observed along the axial direction. The values are within the permissible range and insignificant to cause vibration, chatter and sudden breakage of the tool. A significant increase in the moment of the cutting force can cause the fretting of the tool and spindle taper, thus, resulting in undesirable tool and work piece deflection or bending. This will promote dimensional inaccuracy of the final product with decrease in the tool life. An increase in the tool length with high cutting force will create excessive side load with resulting large torque thereby causing the tool and work piece to bend. This implies that the cutting force is an important cutting parameter that should be kept within the optimum range in order to enhance effective rate of material removal without vibration or chatter.

Table 4. Combination of process parameters and the corresponding cutting forces.

Run	Cutting speed (mm/min)	Feed per tooth (mm)	Depth of cut (mm)	Radial cutting force Fy (N)	Tangential cutting force Fx (N)	Axial force fz (N)	Moment of force My (Nm)	Moment of force Mx (Nm)	Moment of force Mz (Nm)
1	267.50	0.24	1.75	12.62451	14.67488	13.46789	-2.93	2.82	2.84
2	270	0.04	1.50	11.77002	16.24650	13.79850	-2.97	2.67	2.86
3	267.50	0.14	1.40	11.95313	15.20157	12.54667	-3.15	3.08	2.61
4	265	0.20	0.50	10.30578	17.37894	15.66570	-3.37	2.97	2.82
5	275	0.20	3.00	10.91553	20.47869	12.11560	-2.93	2.67	2.77
6	260	0.14	1.65	11.52588	25.56740	20.44567	-3.26	2.86	2.77
7	267.50	0.06	2.00	11.28174	21.87740	15.23470	-2.86	2.82	2.83
8	260	0.08	1.65	10.85449	23.80533	9.223560	-2.67	2.67	2.88
9	265	0.12	1.00	10.18311	23.80533	8.058990	-3.11	2.71	2.88
10	270	0.16	1.75	11.28174	18.67768	14.05683	-3.26	2.60	2.80
11	275	0.08	0.50	11.40381	22.09540	9.675690	-3.08	2.71	2.77
12	254.89	0.06	0.30	12.07520	19.98530	13.34560	-3.11	2.60	2.82
13	260	0.20	0.60	12.50244	22.58790	13.87943	-2.86	2.71	2.83
14	265	0.22	2.40	12.31934	24.97405	19.39856	-3.08	2.49	2.78
15	270	0.14	2.50	11.83105	21.78000	12.09465	-3.41	2.93	2.86
16	275	0.16	2.80	11.64795	22.09830	15.93457	-3.22	2.97	2.73
17	265	0.18	2.60	11.46484	21.67020	16.04768	-3.30	3.04	2.80
18	260	0.14	1.60	10.61035	16.48975	15.98560	-3.22	2.64	2.70
19	267.50	0.16	1.55	10.5493	19.88765	19.00002	-3.26	2.89	2.78
20	280.11	0.10	2.50	11.55678	20.00054	19.86735	-2.86	2.75	2.92

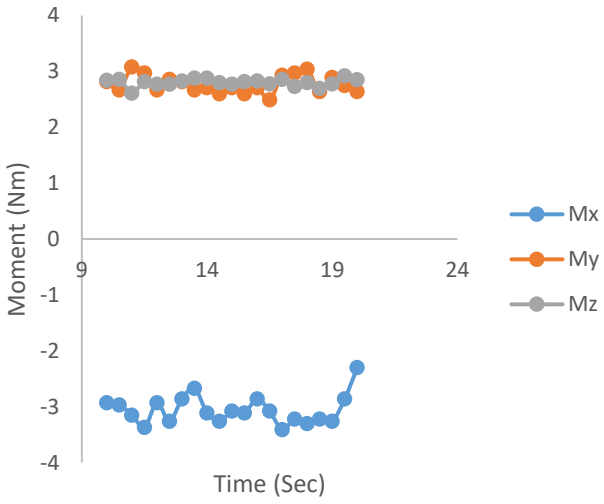

Fig. 8. The variation of the moment of the cutting forces within 20 seconds.

Fig. 9 shows the resultant moment of the cutting forces along the different cutting angles. The magnitude of the resultant cutting force was insignificant from angles 0° to 60° and from angles 0° to 270° but was significant from angles 60° to 270°. The resultant moment should be kept below the threshold in order to avoid a catastrophic failure of the tool.

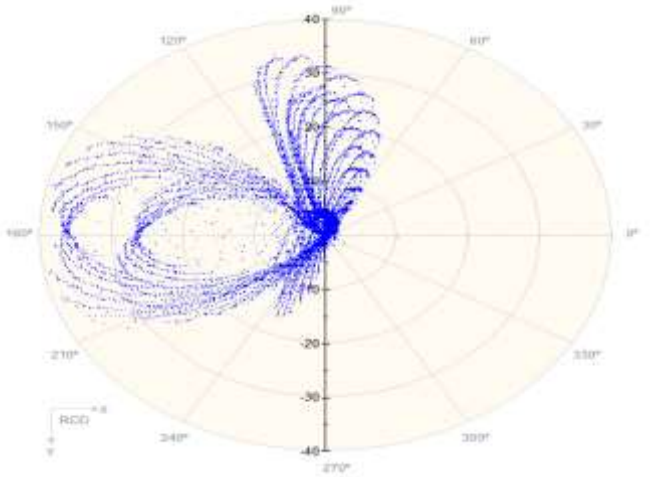

Fig. 9. The resultant moment of forces at different angles.

4. Conclusion

This study highlights the various methods to improve the machinability and surface finish of titanium alloy. These methods include; the use of pCBN and PCD tools, cooling systems, process optimization as well as the design and selection of the proper geometry for the cutting tool. The computer aided design and the finite element analysis was carried out using the solidworks 2016. The results indicate insignificant rate of material removal due to low cutting force. The physical experiments show that the variation of values of the process parameters affect the magnitude of the cutting force significantly along the tangential, radial and axial directions. Hence, the optimization of the process parameters influences

the magnitude of cutting force and promotes the rate of material removal. This work finds application in the manufacturing industry as it provides in depth understanding of the machining characteristics and behaviour of titanium alloy. It is recommended that the optimization of the process parameters for the milling of Ti6Al4V be carried out to determine the optimum range of the process parameters and tool geometry. This will lead to the formulation of mathematical model, which correlates an dependent process parameter (the measured variable) as a function of the independent process parameters.

References

[1] Arrazola, P. J., Garay, A., Iriate, L. M., Armendia, M., Marya, S. and Le Maitre, L. "Machinability of Titanium Alloys (Ti6Al4V and Ti555.3)". *Journal of Materials Processing Technology,* 2009, 209:223-230.

[1] Bandapalli, C., Sutaria, B.M. and Bhatt, D.V. High speed machining of Ti-alloys- A critical review. National Conference on Machines and Mechanisms, 2013, 1(16): 324–331.

[2] Ezugwu, E. O. and Wang, Z. M. Titanium alloys and their machinability – a review, *Journal of Materials Processing Technology*, 1997, 68:262-274.

[3] Rahman, M., Wong, Y. S., and Zareena, A. R. Machinability of Titanium Alloys, *JSME International Journal. Series B, Fluids and Thermal Engineering*, 2003, 46(1):107-115.

[4] Machado, A. R. and Wallbank, J. Machining of titanium and its alloys – a review, *Proceedings of the Institution of Mechanical Engineers. Part B, Journal of Engineering Manufacture*, 1990, 204(12):53.

[5] Arrazola, P. J., Garay, A., Iriate, L. M., Armendia, M., Marya, S. and Le Maitre, L. Machinability of Titanium Alloys (Ti6Al4V and Ti555.3). *Journal of Materials Processing Technology,* 2009, 209:223-230

[6] Haghighi, S. E., Lu, H., Jian, G., Cao, G., Habibi, D. and Zhang, L. Effect of α ″martensite on the microstructure and mechanical properties of beta-type Ti–Fe–Ta alloys, *Mater. Des*. 2015, 76:47–54.

[7] Ehtemam-Haghighi, S., Liu, Y., Cao, G., and Zhang, L.-C. Influence of Nb on the β→ α″martensitic phase transformation and properties of the newly designed Ti–Fe–Nb alloys, *Mater. Sci. Eng.* 2016, 60: 503–510.

[8] Matsushita, T., Kokubo, T. and Matsuda, S. Effect of pore size on bone ingrowth into porous titanium implants fabricated by additive manufacturing: an in vivo experiment, *Mater. Sci. Eng.* 2016, 59:690–701.

[9] Quintana, G. and Ciurana, J. Chatter in machining processes: A review. *International Journal of Machine Tools & Manufacture,* 2011, 51(5): 363–376.

[10] Abele. E. High speed milling of titanium alloys" *Advances in Prod. Eng. & Mgt.*, 2008, 3(3):131-140.

[11] Jaffery, S. and Mativenga, P. Assessment of the machinability of Ti-6Al-4V alloy using the wear map approach. *The International Journal of Advanced Manufacturing Technology,* 2009, 40, 687-696.

[12] Habrat, W., Motyka, M., Topolski, K. and Sieniawski, J. Evaluation of the cutting force components and the surface roughness in the milling process of micro- and nanocrystalline titanium. *Arch. Metall. Mater.,* 2016, 61 (3):1379–1384.

[13] U.S. Titanium Industry Inc.. Titanium Alloys - Ti6Al4V Grade 5. AzoM, 2017. Retrieved on July 02, 2019.

[14] Benedetti, M., Cazzolli, M., Fontanari, V. and Leoni, M. Fatigue limit of Ti6Al4V alloy produced by selective laser sintering, *Procedia Structural Integrity,* 2016, 2: 3158–3167.

[15] Nurul, A. K. M. Effectiveness of incoated WC-CO and PCD inserts in end milling of Ti alloy, *Journal of Materials Processing Technology*, 2007, 192-193:147-158.

[16] Singh, R. (n.d). ME 338: Manufacturing Processes II. pp. 1-59.

[17] Yang, X. and Liu, C. R. Machining Titanium and its Alloys, *Machining Science and Technology*, 1991, 3(1):107- 139.

[18] Arrazola, P. J., Garay, A., Iriate, L. M., Armendia, M., Marya, S. and Le Maitre, L. "Machinability of Titanium Alloys (Ti6Al4V and Ti555.3)". *Journal of Materials Processing Technology,* 2009, 209:223-230.

[19] Mann, J. B., Guo, Y., Saldana, C., Compton, W. D. and Chandrasekar, S. Enhancing material removal processes using modulation-assisted machining, *Tribology International*, 2011, 44(10):1225-1235.

[20] Daniyan, I. A., Tlhabadira, I., Phokobye, S. N., Siviwe, M. and Mpofu, K. Modelling and optimization of the cutting forces during Ti6Al4V milling process using the Response Surface Methodology and dynamometer. *MM Science Journal,* 2019, pp. 3353-3363.

[21] Bello, E. I., Ogedengbe, T. I., Lajide L, Daniyan, I. A. Optimization of process parameters for biodiesel production using response sur-face methodology. *Am J. Energy Eng.,* 2016, 4(2):8–16.

[22] Enweremadu, C.C. and Rutto, H. L. Optimization and modeling of process variables of biodiesel production from marula oil using response surface methodology. *Journal of the Chemical Society of Pakistan*, 2015. **37**(2): p. 256-265.

[23] Salamatinia, B., I. Hashemizadeh, and A. Ahmad Zuhairi. Alkaline earth metal oxide catalysts for biodiesel production from palm oil: elucidation of process behaviors and modeling using response surface methodology. *Iranian Journal of Chemistry and Chemical Engineering* (IJCCE), 2013. **32**(1): p. 113-126.

[24] Nurul, A. K. M. Effectiveness of incoated WC-CO and PCD inserts in end milling of Ti alloy, *Journal of Materials Processing Technology*, 2007, 192-193:147-158.

[25] Rashid, R. R., Sun, S., Wang, G., Dargusch M. An investigation of cutting forces and cutting temperatures during laser-assisted machining of the ti-6cr-5mo-5v-4al beta titanium alloy. *Int J Mach Tools Manuf.* 2012, 63:58–69.

[26] Ayed, Y., Germain, G., Salem, W. B., Hamdi, H. Experimental and numerical study of laser-assisted machining of Ti6Al4V titanium alloy. *Finite Elem Anal Des.* 2014, 92:72–79.

[27] Priyadarshini, A., Pal, S. K. and Samantaray, A. K. Finite element modeling of chip formation in orthogonal machining. In Statistical and computational techniques in manufacturing, Springer, Berlin, Heidelberg, , 2012 pp. 101-144.